

# Influence of the $\beta$ crystalline phase on the mechanical properties of unfilled and $\text{CaCO}_3$ -filled polypropylene. I. Structural and mechanical characterisation

T. Labour<sup>a</sup>, C. Gauthier<sup>a</sup>, R. Séguéla<sup>a,\*</sup>, G. Vigier<sup>a</sup>, Y. Bomal<sup>b</sup>, G. Orange<sup>b</sup>

<sup>a</sup>CNRS Groupe d'Etudes de Métallurgie Physique et de Physique des Matériaux, INSA de Lyon, Bat. 502, 20 avenue Albert Einstein, 69621 Villeurbanne, France

<sup>b</sup>RHODIA, Centre de Recherches d'Aubervilliers, 52 rue de la Haie de Coq, 93308 Aubervilliers, France

Received 4 October 2000; received in revised form 15 January 2001; accepted 26 January 2001

## Abstract

The influence of  $\beta$  crystals on the mechanical properties of isotactic polypropylene is studied on compression-moulded sheets without filler or filled with stearate-coated calcium carbonate particles. A crystallisation procedure is setup for producing sheets with various amounts of  $\beta$  crystals, trying to keep constant crystallinity, spherulite size and crystal thickness. An optimum of  $\beta$  crystals among  $\alpha$  crystals is first produced by isothermal crystallisation at 110°C. Then gradual transformation of  $\beta$  into  $\alpha$  crystals is carried out through thermal annealing at 152°C after an intermediate cooling down to room temperature. Due to the thermal inertia of the large sheet thickness, the amount of  $\beta$  crystals does exceed 10% for unfilled sheets and 50% for filled sheets. Dynamic mechanical behaviour shows that molecular mobility is higher in the  $\beta$  crystals than in the  $\alpha$  crystals, as judged from the temperature of the crystalline relaxation. Loss modulus in the temperature range of the crystalline relaxation also indicates greater damping capacity for the  $\beta$  crystals. This is discussed in terms of activation of conformational defects moving along the chain stems in the crystal. Plane strain compressive testing reveals better ductility for  $\beta$  rich samples. Interpretation is provided using an approach of semi-crystalline polymer plasticity based on dislocation-governed crystallographic slip. Correlation is made with the viscoelastic behaviour through the concept of conformational defects. © 2001 Elsevier Science Ltd. All rights reserved.

**Keywords:** Polypropylene; plasticity;  $\beta$  form

## 1. Introduction

The morphological features of semi-crystalline polymers such as crystallinity level, spherulite size, crystal thickness, etc. are mainly governed by the nature of the polymer which includes chain flexibility, tacticity, short branch bulkiness, long branching frequency and chain length distribution. Crystalline morphology is also strongly sensitive to thermo-mechanical treatment and processing. Number of studies has been devoted to the influence of changes of the morphological parameters on mechanical properties, notably in the case of polypropylene [1–3]. A major problem in probing the property dependency on a given structural parameter is to keep all other parameters constant. Indeed, changing thermal treatment generally involves concomitant modifications of several structural parameters so that the exact origin of property changes is difficult to assign.

Isotactic polypropylene (PP) is well known to simulta-

neously crystallise into two crystalline forms,  $\alpha$  and  $\beta$  [4], their relative amounts being essentially determined by the crystallisation temperature or the cooling rate due to different nucleation and growth rates of the two crystalline species [4–7]. The  $\beta$  phase has been reported to have higher ductility and strength than the  $\alpha$  phase [8–12] with little loss of stiffness [10,11]. However, unless using specific  $\beta$ -nucleating agents, the  $\beta$  phase cannot be obtained at high levels and is always accompanied by  $\alpha$  crystals. Contradictory conclusions, that have appeared among literature data, might be ascribed to insufficient control of the various morphological parameters as the  $\beta/\alpha$  ratio is changed by means of appropriate thermal treatments.

The present work deals with the study of the mechanical properties of PP as a function the  $\beta$  phase concentration, making a particular effort to keep all the other structural parameters constant, namely the overall crystallinity, spherulite size and average crystal thickness. The preparation procedure consists of isothermal crystallisation in the temperature domain of faster  $\beta$  phase crystallisation rate,

\* Corresponding author.

followed by gradual change of the  $\beta$  spherulites into  $\alpha$  spherulites owing to an appropriate thermal annealing. PP filled with  $(\text{CaCO}_3)$  particles coated with a  $\beta$ -nucleating agent has been also studied on the one hand for analysing the combined effect of hard particles and  $\beta$  phase, and on the other hand for optimising the  $\beta$  phase content. Investigations on the impact properties and crack propagation behaviour are reported in an accompanying paper [13].

## 2. Materials and experimental

The polypropylene under investigation is an Eltex PHV001P from Solvay (Belgium) containing 0.2% of Irganox B225 antioxidant. Filled samples were prepared by introducing 10% by weight of stearic acid-coated  $\text{CaCO}_3$  particles during extrusion at  $190^\circ\text{C}$ . The synthetic particles, Calofort S from Rhodia (France), have an average diameter of  $0.1\ \mu\text{m}$  and a surface coating of about 50% by weight. Two kinds of materials have been compression-moulded at  $180^\circ\text{C}$  into sheets 1 or 4 mm thick. The thicker sheets were intended for compressive deformation experiments together with the study of rupture behaviour reported in the accompanying paper [13].

Differential scanning calorimetry (DSC) measurements have been carried out on a Perkin–Elmer DSC 7 at a heating rate of  $10^\circ/\text{min}$ . The temperature and heat capacity scales have been calibrated from the melting scans of high purity indium and zinc samples at the same heating rate. The values of melting enthalpy that were used for determining crystal weight fractions are  $\Delta H_f^0(\alpha) = 145 \pm 10\ \text{J/g}$  and  $\Delta H_f^0(\beta) = 115 \pm 10\ \text{J/g}$ , respectively, for perfect  $\alpha$  and  $\beta$  crystals [7,14,15].

Wide-angle X-ray scattering (WAXS) was performed in reflection mode using the monochromated  $\text{CuK}\alpha$  radiation from a Rigaku generator operated at 40 kV and 25 mA. The  $\beta$  phase fraction in the crystalline part of any specimen was assessed from the ratio of the height of the main (300)  $\beta$  reflection to the sum of the heights of the four main crystalline reflections, i.e. (110), (040) and (130) from the  $\alpha$  phase plus (300) from the  $\beta$  phase, as proposed by Turner-Jones et al. [4]. The various reflection heights were determined after subtraction of the amorphous halo. This  $\beta/(\alpha + \beta)$  ratio is designated in the text as the  $\beta$  phase concentration.

Small-angle X-ray scattering (SAXS) was performed in point collimation configuration owing to two bent nickel-coated glass mirrors at right angles to each other, with three pairs of perpendicular slits for eliminating parasitic scattering. The microfocus incident beam was generated by a Rigaku rotating anode operated at 40 kV and 50 mA. The scattered intensity from the sample placed immediately after the third set of scattering slits was collected on a linear proportional counter located at about 80 cm from the sample. The long periods were computed from the maximum in the scattering intensity profiles of the counter-selected  $\text{CuK}\alpha$  photons.

Dynamic mechanical analyses (DMA) were carried out on a home-built torsion pendulum [16] operating under vacuum at a frequency of 1 Hz. The temperature domain ( $-40$ ;  $+140^\circ\text{C}$ ) was scanned at a heating rate of  $1^\circ/\text{min}$ . The  $G'$  storage and  $G''$  loss moduli were computed at  $2^\circ$  intervals from integrations of the stress and strain functions over four consecutive periods.

Plane strain compressive tests [17] were carried out on an Adame1–Lhomargy DY25 machine equipped with  $8\ \text{mm} \times 25\ \text{mm}$  rectangular dies, at room temperature (RT), using a cross-head speed of  $0.25\ \text{mm}/\text{min}$ . The relative displacement of the dies was measured by means of two capacitive sensors. The 4 mm thick samples were machined out and carefully polished for insuring perfect parallelism of the larger faces in contact with the dies without any lubricating agent.

## 3. Crystallization procedure and control

Borrowing from the profuse literature data on PP crystallisation [4,7,18–21], the schematic time–temperature–crystallisation (TTC) diagram of Fig. 1 may be drawn. The  $\alpha$  phase can be obtained as a unique crystalline component by isothermal crystallisation above  $130^\circ\text{C}$ , whereas in the range  $130$ – $105^\circ\text{C}$ , isothermal crystallisation essentially leads to  $\beta$  phase formation. In this second case, even very fast cooling from the melt down to the  $130$ – $105^\circ\text{C}$  temperature range can hardly be achieved without crossing the tip of the  $\alpha$  phase domain of the TTC diagram. This involves promotion of  $\alpha$  nuclei prior to  $\beta$  phase crystallisation so that  $\alpha$  crystals always coexist with  $\beta$  crystals in the final sample. The thinner the sample, the more efficient is the quenching effect, and the higher is the  $\beta$  content. Nucleating agents, such as calcium stearate [7], can however be used for enlarging the temperature domain of  $\beta$  phase

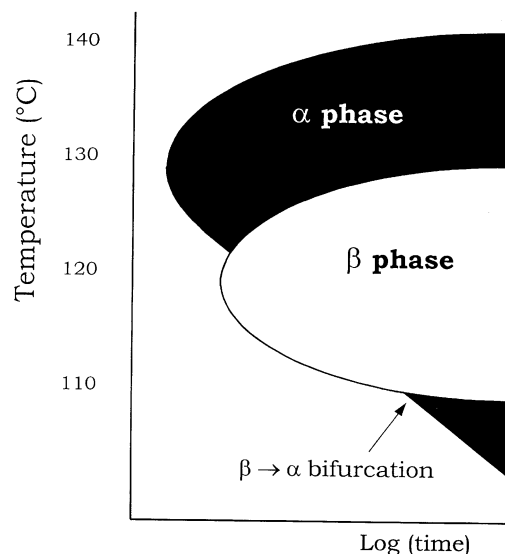


Fig. 1. Schematic time–temperature–crystallisation diagram of iPP.

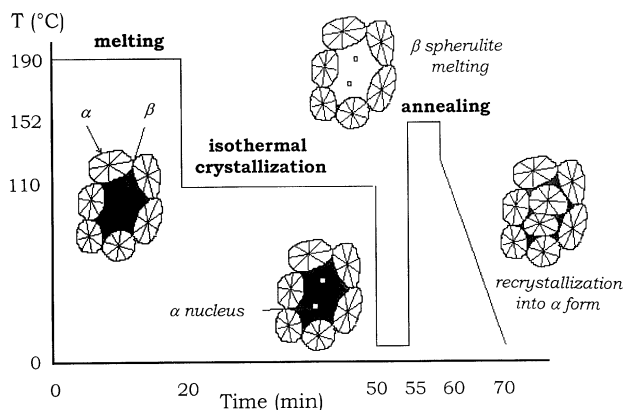


Fig. 2. Synoptic path of sample crystallisation in the TTC diagram.

crystallisation and improving the corresponding  $\beta/\alpha$  crystal ratio, notably for bulk samples.

According to the above TTC diagram of PP, a specific crystallisation procedure has been setup for producing samples having various  $\beta/\alpha$  crystal ratios with expected constant crystallinity and spherulite size. Fig. 2 displays the synoptic pathway of this procedure. After being held in the molten state for 20 min at 200°C, the sample is quickly plunged into a silicone oil bath in the temperature range 110–135°C, for an isothermal crystallisation of 30 min. Variable proportions of  $\beta$  spherulites surrounded by  $\alpha$  spherulites can be obtained depending on the chosen temperature. The maximum amount of  $\beta$  phase was obtained for a temperature of 125°C in the case of 1 mm thick sheets. The sample is subsequently cooled down in air at RT for 5 min. This step generates  $\alpha$  nuclei at the interspherulite boundaries [7,21], due to the  $\beta \rightarrow \alpha$  crystallisation bifurcation below 105°C (Fig. 1). The sample is then quickly heated up to 152°C, i.e. just about the melting peak temperature of the  $\beta$  phase, and annealed at this temperature for a few minutes before being rapidly cooled down to RT. This treatment allows gradual melting of the  $\beta$  spherulites that readily recrystallise into  $\alpha$  spherulites about the  $\alpha$  nuclei. The amount of  $\beta$  phase remaining at the end of the annealing at 152°C essentially depends on the treatment duration.

In the case of the 4 mm thick sheets, the procedure was slightly modified by lowering the isothermal temperature to 110°C. Indeed, due to the strong thermal inertia of the samples, a compromise should be made between optimum crystallisation temperature and faster cooling rate in order to get as much  $\beta$  phase as possible in the core of the sheets.

The procedure has been tested using DSC experiments. Fig. 3 shows the incidence of the temperature of the isothermal crystallisation treatment for 30 min, in the case of unfilled samples. A maximum of 10% of  $\beta$  phase is clearly obtained for 125°C as judged from the amplitude of the  $\beta$  melting peak at about 150°C, and the overall weight crystallinity is close to 65%. The filled samples display similar melting behaviour, the maximum  $\beta$  phase content being

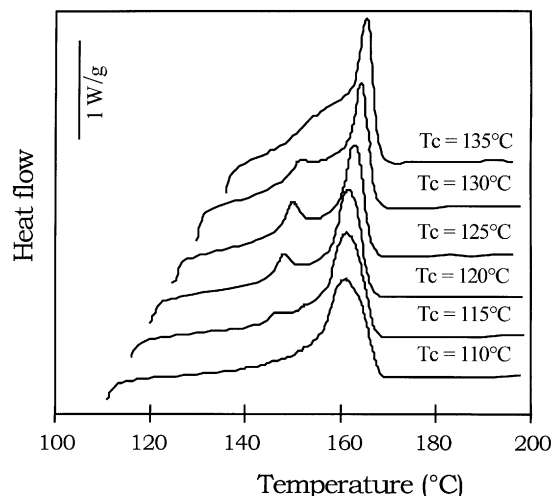


Fig. 3. DSC melting curves of unfilled samples isothermally crystallised for 30 min at various temperatures.

about 50% owing to the nucleating effect of the stearate coating of the  $\text{CaCO}_3$  particles.

The size of the  $\alpha$  spherulites formed during the isothermal crystallisation is only slightly sensitive to crystallisation temperature, as well as the annealing duration and temperature, as far as this latter does not exceed 152°C. The  $\alpha$  spherulites formed from the re-crystallisation of the  $\beta$  spherulites melted at 152°C have about the same size as the other  $\alpha$  spherulites since, on the one hand, the original  $\beta$  spherulites are about twice as large as the  $\alpha$  ones due to greater growth rate and, on the other hand, every  $\beta$  spherulite gives rise on average to two  $\alpha$  ones. Fig. 4 is an example of an optical micrograph of the acid-etched surface of an unfilled PP sheet isothermally crystallised at 125°C showing rugged  $\alpha$  and smooth  $\beta$  spherulites with diameters in the range 30–50  $\mu\text{m}$ . The concavity of the  $\beta$  spherulite edges compared with the edge convexity of the  $\alpha$  spherulites gives clear evidence of the higher growth rate of the  $\beta$  phase.

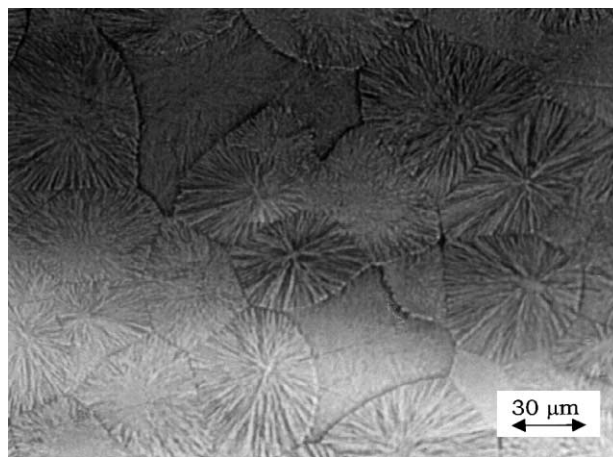


Fig. 4. Optical micrograph of acid-etched unfilled bulk sample isothermally crystallised at 110°C for 30 min.

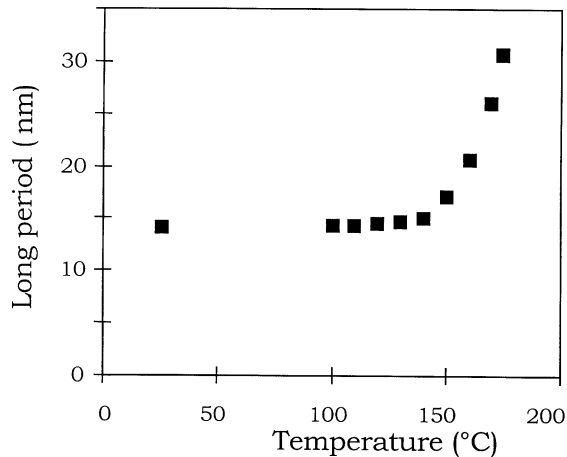


Fig. 5. SAXS long periods measured as a function of temperature for an unfilled sample isothermally crystallised for 30 min at 125°C (see text for experimental details).

Following isothermal annealing at 152°C, the overall crystallinity level assessed from DSC was about  $65 \pm 2\%$  for both unfilled-PP and filled-PP, irrespective of the annealing duration. Similar figures have been obtained from WAXS. This confirms our expectation that the liquid pockets resulting from the  $\beta$  phase melting at 152°C should gradually recrystallize into  $\alpha$  phase thanks to the  $\alpha$  nuclei generated during the intermediate cooling step at RT, without significant additional crystallisation from the remaining amorphous phase, owing to the short time treatment.

Lamellar thickness assessed from SAXS long periods and DSC crystallinity data is about 10 nm. This value roughly holds for both crystal species as judged from the long periods of Fig. 5 showing only a very slight change in the temperature domain RT – 130°C before the melting of the  $\beta$  crystals. There is however some change in long period above 130°C corresponding to a crystal thickening process during the time of the experiment, i.e. about 1 h at a heating rate of 2°/min, the recording time of every SAXS profile being 1 min. One may suspect the  $\beta$  crystals to be more involved in this process than the  $\alpha$  crystals since the latter have been grown at higher temperature. This thickening does not seem to have a significant effect on the mechanical properties as will be seen later.

The DSC melting curves of Fig. 6 show the determining part of the cooling step prior to the annealing at 152°C. For the sample that has been cooled down to 90°C for 5 min (Fig. 6a), i.e. just 15° below the  $\beta \rightarrow \alpha$  bifurcation temperature, after the isothermal crystallisation at 125°C, not any sign appears of the  $\beta$  melting peak at about 150°C, only the  $\alpha$  melting occurs at about 165°C. As a matter of fact, the annealing for 10 min at 152°C has involved melting of the  $\beta$  crystals, and a complete recrystallisation of the molten material into  $\alpha$  crystals has occurred during the final cooling

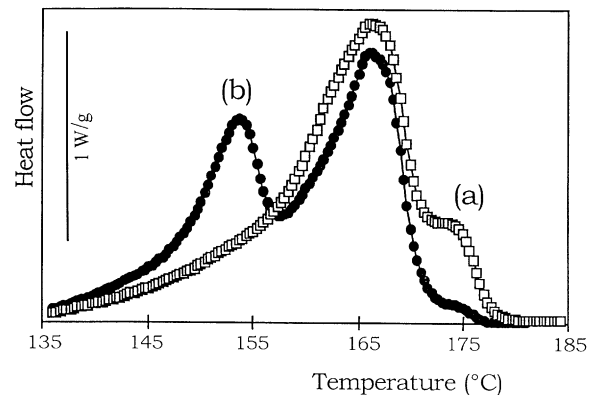


Fig. 6. DSC melting curves of unfilled samples isothermally crystallised for 30 min at 125°C and subsequently annealed at 152°C for 10 min; (a) with intermediate quick cooling down to 90°C for 5 min and (b) without intermediate cooling.

thanks to the  $\alpha$  nuclei promoted during the 90°C annealing. In contrast, the sample not annealed at 90°C (Fig. 6b) displays a strong  $\beta$  melting peak indicating that the  $\beta$  crystals that have necessarily melted during the annealing at 152°C have reformed during the final cooling step.

It is worth noticing that an additional melting occurred in the range 170–180°C (Fig. 6a). This is seemingly due to some  $\alpha$  crystals that have thickened or turned more perfect during the annealing at 152°C. In our aim for trying to maintain all structural parameters constant, during the  $\beta \rightarrow \alpha$  transformation, this drawback could be easily avoided by limiting to 5 min the annealing time at 152°C.

The duration of the 152°C annealing is a determining parameter for the amount of remaining  $\beta$  phase as can be seen on the WAXS patterns of Fig. 7, in the case of filled samples. The amount of  $\beta$  phase crystals in the whole crystalline component gradually drops as annealing time increases. All the  $\beta$  crystals have disappeared after 5 min treatment at 152°C.

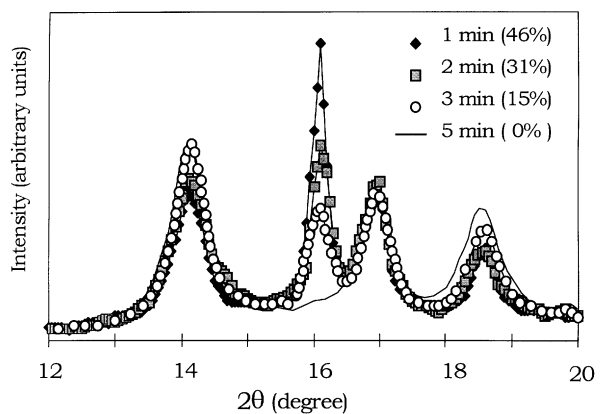


Fig. 7. WAXS intensity profiles of filled samples crystallised following the procedure described in Fig. 2, for various annealing times at 152°C.

## 4. Mechanical properties

### 4.1. Dynamic mechanical analysis

The storage modulus data versus temperature obtained from mechanical spectroscopy do not reveal reliable differences that could be ascribed to the changes in  $\beta$  phase content due to thermal treatment, for both unfilled and  $\text{CaCO}_3$ -filled samples. Notwithstanding, the previously reported nano-indentation experiments [22] clearly show that the  $\beta$  spherulite elastic modulus at RT is about 8% lower than that of the  $\alpha$  spherulites, as already reported by various authors [8,10,11] from tensile testing.

In contrast, the loss modulus and loss factor data are particularly sensitive to  $\beta$  phase changes. Fig. 8 shows the loss modulus variations with temperature for unfilled-PP and filled-PP having various amounts of  $\beta$  phase. In both cases, the rather broad and flat  $G''$  peak due to the activation of mechanical relaxation in the crystalline component, in the range 60–100°C, is gradually shifted to lower temperature as the  $\beta/\alpha$  ratio increases. This is relevant to an improved mechanical absorption in the low temperature region of the crystalline relaxation due to the  $\beta$  phase, i.e. the relaxation peak of the  $\beta$  phase should occur at lower temperature than that of the  $\alpha$  phase. Unfortunately, the respective relaxation maxima of the two crystalline phases cannot be resolved,

owing to the typical broadness of this kind of relaxation. Notwithstanding, considering that the crystalline relaxation in most flexible-chain semi-crystalline polymers is ascribed to the migration of conformational defects along the chain stems through the crystallite thickness [23], and notably in the case of PP [16], the observed shift to lower temperature clearly indicates an easier activation of chain mobility in the  $\beta$  crystalline lamellae as compared to the  $\alpha$  ones.

In parallel, the  $G''$  relaxation peak associated with the glass transition of the amorphous phase (Fig. 8a and b), at about 10°C, inversely decreases in amplitude with the  $\beta$  phase content. Considering that crystallinity and average spherulite size remain roughly constant as the  $\beta$  content changes, for unfilled-PP as well as for filled-PP, this phenomenon may be ascribed to a modification of the mechanical coupling between the crystalline and amorphous phases through the stiffness change in the crystalline component. Indeed, as the concentration of the more compliant  $\beta$  form increases in the crystalline component, this latter gradually turns less stiff and more deformable. This is accompanied by a weaker mechanical response from the amorphous component which results in a reduced amplitude of its main damping peak. It is worth noticing that Jacoby et al. [8] and Crissman [24] have both reported a so-called increase in the amorphous relaxation peak with increasing  $\beta$  phase content. Their data indeed show an increase in the damping value at the peak that may be ascribed to the shift to lower temperature of the crystalline relaxation, but the damping amplitude of the amorphous relaxation actually decreases, as observed from our data.

The faint, but systematic, shift to higher temperatures of the glass transition relaxation as the  $\beta$  content increases (Fig. 8a and b) is indicative of a slight chain immobilisation in the amorphous phase in the vicinity of the  $\beta$  phase lamellae. This might be ascribed to more numerous tie chains through the amorphous layers located between  $\beta$  lamellae than the ones between  $\alpha$  lamellae for reasons of faster crystallisation kinetics of the  $\beta$  phase as has been suggested by some authors [8,11].

The loss factor data reported in Fig. 9 reveal a systematic increase of mechanical damping in the temperature domain of the crystalline relaxation as the  $\beta$  phase content increases. This is evidence for a higher damping capacity of the  $\beta$  phase, compared with the  $\alpha$  phase, which obviously results from the above-mentioned easier activation of chain mobility in the  $\beta$  phase. This point, together with the concomitant slight drop of the amorphous phase damping peak amplitude, thoroughly supports the assumption of a modified mechanical coupling due to stiffness changes in the crystalline component.

It is well known that the peak temperature of crystalline relaxation in semi-crystalline polymers depends mainly on crystal thickness [25,26]. Indeed, at a given frequency, thicker crystal lamellae require higher thermal activation for allowing faster migration of conformational defects over the whole crystal thickness. In the present case, the

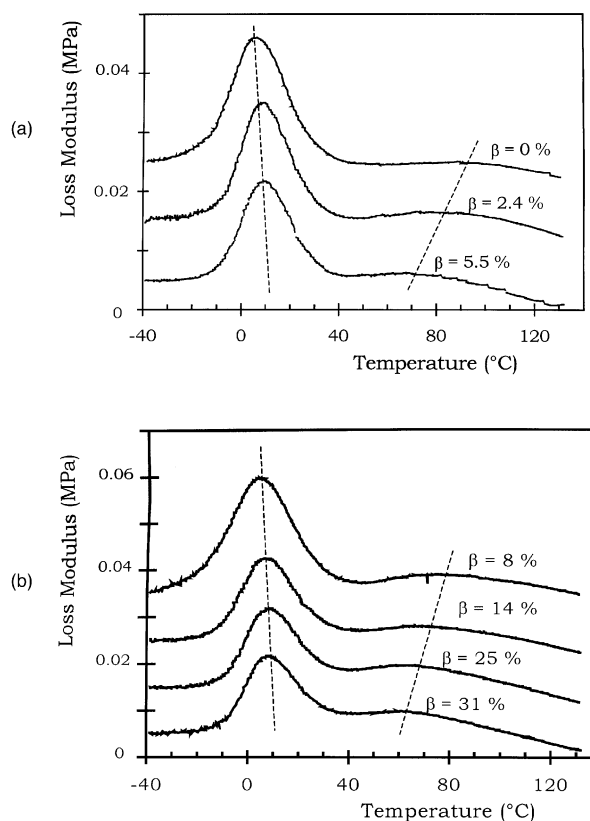


Fig. 8. Loss modulus,  $G''$ , versus temperature of (a) PP and (b) filled-PP samples having various concentrations of  $\beta$  phase (the Y scale refers to the lower curve and the other curves are arbitrarily shifted upward).

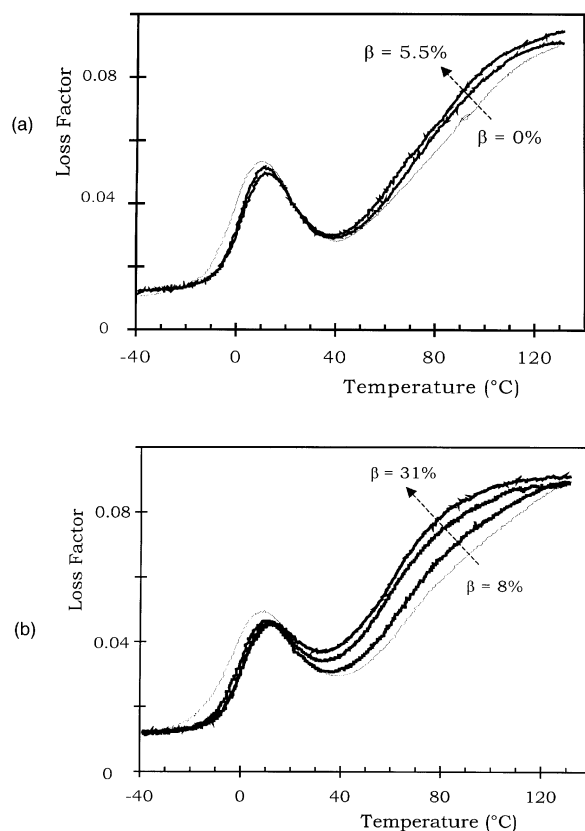


Fig. 9. Loss factor,  $\tan\delta$ , versus temperature of (a) PP and (b) filled-PP samples having various concentrations of  $\beta$  phase.

lower relaxation temperature of the  $\beta$  crystals compared with  $\alpha$  crystals, that is responsible for the shift to lower temperature of the broad crystalline relaxation (Fig. 8), cannot be ascribed to a lower crystal thickness of the  $\beta$  crystal species. One may however reasonably suspect the 3% lower packing density of the  $\beta$  phase [4] to involve reduced chain interactions in the  $\beta$  crystalline lamellae as compared to the  $\alpha$  lamellae, an assumption that is thoroughly supported by the 25% lower melting enthalpy of the  $\beta$  phase. In the present case of isotactic PP, the most probable conformational defect in the 3/1 helix of the crystalline stems is a  $120^\circ$  chain twist accompanied with a  $c/3$  shift in the stem direction [27–29]. It is obvious that lower chain interactions reduce the energy barrier to the rotation-translation jumps of such conformational defects along the chain stems, involving thus a depression of the crystalline relaxation temperature of the  $\beta$  phase with respect to the  $\alpha$  phase, at the same frequency.

#### 4.2. Plastic behaviour

In the previous nano-indentation study [22], the local hardness of the  $\beta$  phase spherulites turned out to be 12% lower than that of the  $\alpha$  phase spherulites. Considering that hardness relies on a complex combination of elasticity and plasticity [30], indentation depth has been chosen in order to

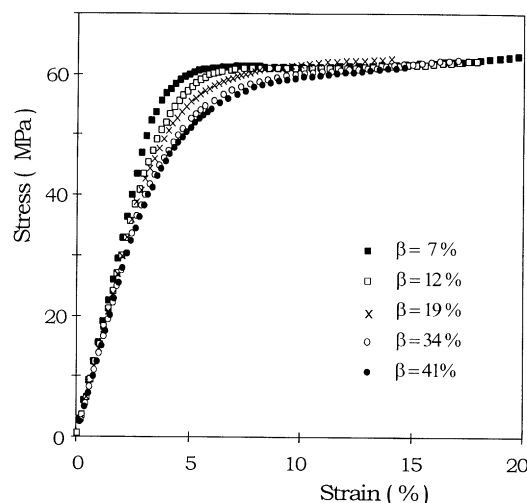


Fig. 10. Nominal stress–strain curves in plane strain compression at RT of filled-PP having as a function of the  $\beta$  phase content.

involve a large component of plastic strain. In these circumstances, the 12% difference in hardness gives clear evidence of a greater plasticity of the  $\beta$  crystalline species.

Stress–strain data from plane strain experiments carried out at RT are reported in Fig. 10 for filled-PP sheets. For an initial strain rate of  $10^{-3} \text{ s}^{-1}$ , RT is above the main relaxation of the amorphous phase so that plastic flow may be mainly ascribed to the crystalline phase. The flow stress in the plateau region, i.e. about 10–15% strain, is surprisingly insensitive to the change in composition of the crystalline phase at nearly constant crystallinity. The initial elastic strain domain is also relatively insensitive, at first glance, to the crystalline form. As a matter of fact, the elastic modulus change discussed above involves only very faint variations of the initial slope of the curve that cannot be clearly distinguished in Fig. 10. The main differences in the  $\sigma(\epsilon)$  curves occur in the intermediate strain domain where the plastic processes are initiated. The transition from the elastic to plastic flow domain is more gradual as the  $\beta$  phase content increases. It is worth noticing that a reduced trend to plastic instability has been reported in tensile testing [11,12]. Owing to the difficulty of determining the onset of non-linearity, an arbitrary elasticity limit at 0.5%,  $EL_{0.5}$ , can be assessed, as commonly made for metallurgic materials, at the stress level where the actual  $\sigma(\epsilon)$  curve departs by 0.5% strain from the extrapolated linear elastic behaviour. The corresponding data reported in Fig. 11 show a clear-cut drop of  $EL_{0.5}$  with increasing  $\beta$  phase content. This is relevant to an early and more gradual activation of plastic processes in the  $\beta$  phase as compared to the  $\alpha$  phase due to easier molecular mobility in the former, at the same temperature.

It is however surprising that the materials become much alike in the plastic flow domain (Fig. 10). The strain-induced  $\beta \rightarrow \alpha$  transition upon tensile drawing, which has been reported by several authors [7,10,31–35], could

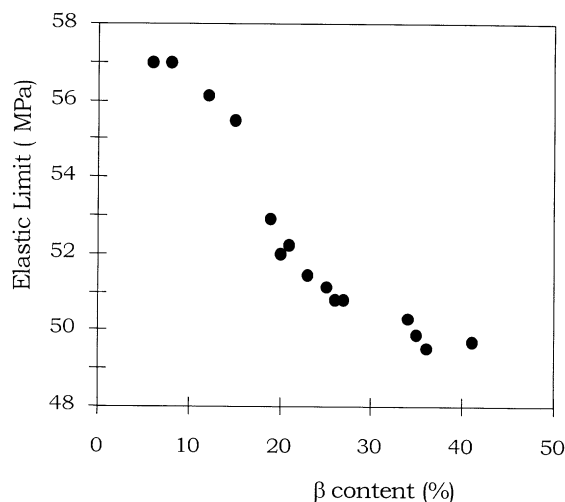


Fig. 11. Elasticity limit at RT for filled-PP as a function of  $\beta$  phase content.

perfectly account for this behaviour. In this case, one may wonder if the benefit of the better ductility of the  $\beta$  phase is not quickly lost upon yielding. But the fact is that  $\beta$ -rich samples display significantly greater strain-hardening in the post-yield range [8,10,32,33], i.e. after the phase transition which seems to be a phenomenon that accompanies chain-unfolding during the fibrillar transformation [31,35]. This may be taken evidence of a memory effect of the  $\beta$  phase after the  $\beta \rightarrow \alpha$  transition in relation to an originally higher tie chain density. This point, which has been already mentioned in Section 4.1, will be further discussed in Section 5.

Plane strain compressive experiments have been performed below the glass transition temperature in order to check if the amorphous phase plays some part in the mechanical modifications brought about by changes in the  $\beta/\alpha$  ratio. Comparison of stress–strain curves at  $-40$  and  $20^\circ\text{C}$  is made in Fig. 12 for samples having 5 and 30% of  $\beta$  phase. It is to be noticed that the flow stress is about quite the same for the two kinds of samples at  $-40^\circ\text{C}$  as already observed for RT. These flow stress values are besides remarkably close to the data reported for uniaxial compression of PP consisting of  $\alpha$  phase only, at the same temperatures [36]. Apart from the increase in stress level due to the drastic change of temperature, the difference between the two kinds of samples is preserved, namely the  $\beta$ -rich sample exhibits a more gradual transition between elastic and plastic behaviour. This is a piece of evidence that the plastic behaviour is much more sensitive to the change of nature of the crystalline phase than to any modification of the chain mobility in the amorphous phase induced by the crystallisation procedure, as indicated in Section 4.1.

For a better insight into the plastic behaviour of the crystalline component, plane strain experiments have been performed in the temperature range of activation of the molecular motions in the crystalline lamellae. Fig. 13

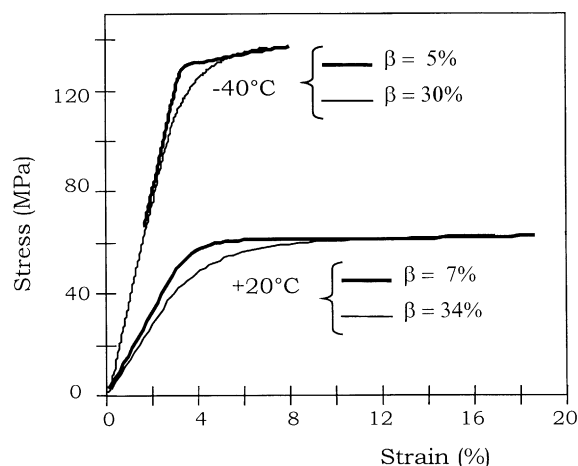


Fig. 12. Nominal stress–strain curves in plane strain compression at 20 and  $-40^\circ\text{C}$  for filled-PP having 5 and 30% of  $\beta$  phase.

shows the stress–strain curves of filled-PP samples having 0 and 25% of  $\beta$  phase, in the region of the yield point, at various temperatures about the crystalline relaxation. For all temperatures, the stress–strain curves of the  $\beta$ -rich sample depart from those of the sample with no  $\beta$  crystals at a strain of about 2%. This corroborates the previous conclusion of an easier stress-activation of the molecular mobility in the  $\beta$  phase as compared to the  $\alpha$  phase. Nonetheless, at 64 and  $76^\circ\text{C}$ , where both the  $\alpha$  and  $\beta$  phases are either below (viz.  $64^\circ\text{C}$ ) or above (viz.  $76^\circ\text{C}$ ) their main relaxation peak, the flow stress of the  $\beta$ -rich sample is about 1 MPa lower than that of the sample with only  $\alpha$  crystals. In contrast, at 68 and  $72^\circ\text{C}$ , where the  $\beta$  phase is more likely to be

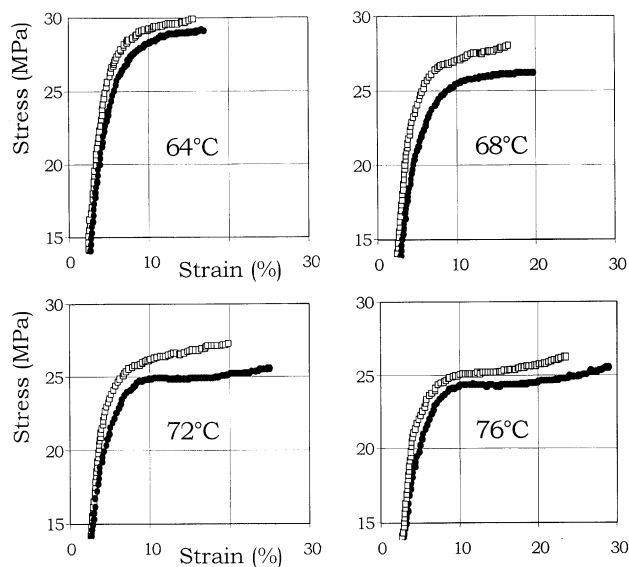


Fig. 13. Nominal stress–strain curves in plane strain compression in the region of the yield point for filled-PP having 0 and 25% of  $\beta$  phase, for various temperatures in the range of the crystalline relaxation.

above its own relaxation peak whereas the  $\alpha$  phase is below its own relaxation peak, the stress gap is more than 2 MPa. Although small, this increase of flow stress gap is evidence for the additional thermal activation of chain mobility in the  $\beta$  phase above its relaxation temperature, which occurs before that of the  $\alpha$  phase.

## 5. Concluding discussion

It has been assumed that cross-hatching of the lamellae in  $\alpha$  spherulites of PP increases stiffness and resistance to plastic flow, as compared to  $\beta$  spherulites [9]. This must certainly hold true for the stiffness since cross-hatching builds up a physical network of the crystalline lamellae which makes the phase mechanical coupling much closer to a parallel (i.e. Voigt model) than to a series association (i.e. Reuss model), so that the overall elastic behaviour of the composite material is close to that of the stiffer crystalline component.

Regarding the inelastic properties, if cross-hatching had some influence, one should expect a reduced mechanical absorption from the soft amorphous phase in the case of  $\alpha$  spherulites with interconnected crystalline lamellae than in the case of  $\beta$  spherulites without interconnection, at equivalent moduli of the soft amorphous and stiff crystalline phases. What is observed is just the contrary, i.e. the loss modulus amplitude near  $T_g$  drops as the  $\beta/\alpha$  ratio increases. We ascribed this phenomenon to an improved mechanical involvement of the amorphous phase due to the reduced stiffness of the  $\beta$  phase as compared with the  $\alpha$  phase.

Regarding the plastic behaviour, it has been clearly shown by Aboulfaraj et al. that  $\alpha$  spherulites deform significantly less than  $\beta$  spherulites well beyond the yield point, i.e. at a strain level for which the junctions of the cross-hatched lamellae should be broken. This is evidence that the intrinsic mechanical properties of the crystalline lamellae are more likely to be involved in the plastic behaviour than their arrangement.

It has been shown in Section 4.1 that molecular motions are more easily activated in the  $\beta$  crystalline phase than in the  $\alpha$  phase, as judged from the peak temperature of the crystalline relaxation. The lower packing density of the  $\beta$  phase, accompanied by reduced chain interactions, is suggested to be the main factor affecting this improved chain mobility. Indeed, conformational chain defects responsible for the crystalline mechanical relaxation should be more mobile in an environment of lower molecular cohesion. This lower cohesion in the  $\beta$  phase may also contribute to the lower elastic modulus.

Such modification of chain mobility in the crystal is likely to modify the plastic properties. Indeed, considering the approach of semi-crystalline polymer plasticity based on dislocation-governed crystal slip, that seems to apply to PP [37,38], dislocation motion is assumed to rely on the activation of conformational defects of the kind proposed for the crystalline relaxation [29,39,40]. The improved

ductility of  $\beta$  PP compared with  $\alpha$  PP is thus associated with the greater chain mobility in the  $\beta$  crystals. In addition, the higher damping capacity of the  $\beta$  phase (i.e. higher loss factor) in the temperature range of its crystalline relaxation suggests a significantly larger concentration of conformational defects in this phase, at equivalent deformation conditions, which is a major factor for plasticity improvement.

An additional factor that should help in reducing resistance to plastic flow initiation is the crystallographic symmetry of the hexagonal  $\beta$  phase providing three equivalent glide planes. This indeed offers a greater probability of favourably orientated crystals for slip with regard to the principal shear stress, and allows a more uniform deformation of the  $\beta$  lamellae at reduced yield stress.

The amorphous phase has also been suspected to have a part in the plasticity modification of PP containing  $\beta$  phase crystals through the intercrystalline tie chain density [8,11]. As a matter of fact,  $\beta$  crystallites are generally grown at lower crystallisation temperature than  $\alpha$  crystallites, i.e. with faster crystallisation kinetics (as far as this occurs well above the glass transition). This is likely to promote more random chain folding with numerous tie chains in the  $\beta$  phase as crystallisation proceeds in the so-called regime III [14,41]. The amorphous phase is thus believed to provide a more uniform stress distribution over the crystalline lamellae in the case of the  $\beta$  phase. This difference of chain topology in the amorphous layers surrounding the two kinds of crystalline phases may be the origin of the higher strain-hardening of  $\beta$  PP that has been observed upon drawing in the post-yield domain, as compared with  $\alpha$  PP. This phenomenon is indeed relevant to a greater resistance to plastic deformation of the microfibrils issued from  $\beta$  spherulites and is responsible for the reduced propensity of  $\beta$  PP for plastic instability. In an investigation of the crazing behaviour of polyoxymethylene thin films by transmission electron microscopy, Plummer and Kausch [42] have shown that low temperature crystallisation leads to a higher entanglement density than high temperature crystallisation that provides better ability for shear deformation versus crazing. The same authors have drawn an analogous conclusion for PP thin films [43]. In addition, they showed different deformation trends for  $\alpha$  and  $\beta$  spherulites, the former being more craze-prone than the latter.

The chain topology features that seem to play a determining part in the deformation behaviour will be further discussed in the accompanying paper concerned with ductile crack propagation and impact strength of unfilled and filled PP as a function of  $\beta$  phase content [13].

## Acknowledgements

The authors are indebted to Rhodia for their financial support of this work and for the grant of a doctoral research fellowship to T. Labour.



## References

- [1] Reinshagen JH, Dunlap RW. *J Appl Polym Sci* 1976;20:9–24.
- [2] Schultz JM. *Polym Engng Sci* 1984;24:770–85.
- [3] Boyd RH. *Polymer* 1985;26:323–47.
- [4] Turner-Jones A, Aizlewood JM, Beckett DR. *Makromol Chem* 1964;75:134–58.
- [5] Lovinger AJ, Chua JO, Gryte CC. *J Polym Sci, Polym Phys* 1977;15:641–56.
- [6] Varga J. *J Mater Sci* 1992;27:2557–79.
- [7] Varga J. Polypropylene structure, blends and composites. In: Karger-Kocsis J, editor. *Structure and morphology*, vol. 1. London: Chapman & Hall, 1995. p. 56–115.
- [8] Jacoby P, Berstedt BH, Kissel WXJ, Smith CE. *J Polym Sci, Polym Phys* 1986;24:461–91.
- [9] Aboulfaraj M, G'Sell C, Ulrich B, Dahoun A. *Polymer* 1995;36:731–42.
- [10] Karger-Kocsis J, Varga J. *J Appl Polym Sci* 1996;62:291–300.
- [11] Tjong SC, Shen SJ, Li RKY. *Polym Engng Sci* 1996;36:100–5.
- [12] Tjong SC, Shen SJ, Li RKY. *Polymer* 1996;37:2309–16.
- [13] Labour T, Gauthier C, Séguéla R, Vigier G, Orange G, Bomal Y. Submitted for publication.
- [14] Monasse B, Haudin J-M. *Colloid Polym Sci* 1985;263:822–31.
- [15] Osawa S, Porter RS. *Polymer* 1994;35:545–50.
- [16] Jourdan C, Cavaillé J-Y, Perez J. *J Polym Sci, Polym Phys* 1989;27:2361–84.
- [17] Bowden PB, Jukes JA. *J Mater Sci* 1968;3:183–90.
- [18] Padden FJ, Keith HD. *J Appl Phys* 1959;30:1472–84.
- [19] Norton DR, Keller A. *Polymer* 1985;26:704–16.
- [20] Lotz B, Wittmann J-C. *J Polym Sci, Polym Phys* 1986;24:1541–58.
- [21] Fillon B, Thierry A, Wittmann J-C, Lotz B. *J Polym Sci, Polym Phys* 1993;31:1407–24.
- [22] Labour T, Ferry L, Gauthier C, Hajji P, Vigier G. *J Appl Polym Sci* 1999;74:195–200.
- [23] Boyd RH. *Polymer* 1985;26:1123–33.
- [24] Crissman JM. *J Polym Sci, Polym Phys* 1969;7:389–407.
- [25] Matsuo T, Takayanagi M. *J Macromol Sci, Phys* 1967;B1:407–31.
- [26] Popli R, Glotin M, Mandelkern L. *J Polym Sci, Polym Phys* 1984;407:448.
- [27] Syi J-L, Mansfield ML. *Polymer* 1988;29:987–97.
- [28] Schaefer D, Spiess HW, Suter UW, Fleming WW. *Macromolecules* 1990;23:3431–9.
- [29] Séguéla R, Staniek E, Escaig B, Fillon B. *J Appl Polym Sci* 1999;71:1873–85.
- [30] Balta-Calleja FJ. *Adv Polym Sci* 1985;66:117–48.
- [31] Yoshida T, Fujiwara Y, Asano T. *Polymer* 1983;24:925–9.
- [32] Shi G, Chu F, Zhou G, Han Z. *Makromol Chem* 1989;190:907–13.
- [33] Zhang X, Shi G. *Polymer* 1994;35:5067–72.
- [34] Chu F, Yamaoka T, Kimura Y. *Polymer* 1995;36:2523–30.
- [35] Li JX, Cheung WL. *Polymer* 1998;39:6935–40.
- [36] Porzucek K, Coulon G, Lefebvre J-M, Escaig B. *J Mater Sci* 1989;24:2533–40.
- [37] O'Kane WJ, Young RJ, Ryan AJ. *J Macromol Sci, Phys* 1995;B34:427–58.
- [38] G'Sell C, Dahoun A, Favier V, Hiver J-M, Philippe M-J, Canova GR. *Polym Engng Sci* 1997;37:1702–11.
- [39] Young RJ. *Philos Mag* 1974;30:85–94.
- [40] Séguéla R, Gaucher-Miri V, Elkoun S. *J Mater Sci* 1998;33:1273–9.
- [41] Clark EJ, Hoffman JD. *Macromolecules* 1984;17:878–85.
- [42] Plummer CJG, Kausch H-H. *J Macromol Sci, Phys* 1996;B35:637–57.
- [43] Plummer CJG, Kausch H-H. *Macromol Chem Phys* 1996;197:2047–63.